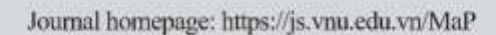


# VNU Journal of Science: Mathematics - Physics





# Original Article

# Temperature-dependent High-order XAFS Cumulants of Gaseous Bromine Calculated Based on the Classical Statistical Theory

Nguyen Thi Minh Thuy<sup>1</sup>, Nguyen To Nu<sup>2</sup>, Nguyen Huy Thao<sup>3</sup>, Tong Sy Tien<sup>1,\*</sup>

<sup>1</sup>University of Fire Prevention and Fighting, 243 Khuat Duy Tien, Thanh Xuan, Hanoi, Vietnam <sup>2</sup>Phong Chau High School, Lam Thao Department of Education, Lam Thao, Phu Tho, Vietnam <sup>3</sup>Hanoi Pedagogical University 2, 32 Nguyen Van Linh, Phuc Yen, Vinh Phuc, Vietnam

> Received 1st April 2025 Revised 28th April 2025; Accepted 20th June 2025

**Abstract:** The anharmonic X-ray absorption fine structure (XAFS) cumulants of gaseous bromine (Br<sub>2</sub>) in an expansion to the  $4^{th}$  order have been calculated under the influence of thermal disorder. The thermodynamic parameters of Br<sub>2</sub> have considered the influence of nearest neighbors on the backscattering and absorbing atoms. The temperature-dependent XAFS cumulants were calculated explicitly and simply from the calculation model developed based on the classical statistical theory within the correlated Einstein model. The obtained numerical results of Br<sub>2</sub> at temperatures from 0 to 600 K fit with those obtained from the experimental XAFS data and other theoretical approaches at various temperatures. These results indicate that the present theoretical model helps analyze experimental XAFS signals of gaseous bromine and other gases.

Keywords: High-oder XAFS cumulants, thermal disorders, gaseous bromine, classical statistics, correlated Einstein model.

## 1. Introduction

Nowadays, many of the thermodynamic properties and structural parameters of materials can be identified using the X-ray absorption fine structure (XAFS) analysis [1-3]. The thermal average of the XAFS oscillation function of a single coordination shell has the form [4]:

E-mail address: tongsytien@yahoo.com

<sup>\*</sup> Corresponding author.

$$\chi(k) = A(k)\sin\Phi(k),\tag{1}$$

where k is the photoelectron wavenumber,  $\Phi(k)$  and A(k) are the XAFS phase and amplitude, respectively.

Normally, the cumulant expansion approach is used to describe anharmonic XAFS oscillations [5]. The formalism of the XAFS function, including anharmonic effects for a single coordination shell, can be represented within the framework of the plane-wave approximations and single-scattering as follows [6]:

$$\chi(k) = F(k) \frac{e^{-2R/\lambda(k)}}{kR^2} \operatorname{Im} \left\{ e^{i\phi(k)} \exp \left[ 2ikR + \sum_{n} \frac{(2ik)^n}{n!} \sigma^{(n)} \right] \right\}, \tag{2}$$

where  $\sigma^{(n)}$  is the *n*-th order cumulant, F(k) is the atomic backscattering amplitude,  $R = \langle r \rangle$  is the average interatomic distance with  $\langle \ \rangle$  denotes the thermal average and r is the instantaneous interatomic distance,  $\phi(k)$  is a net phase shift, and  $\lambda(k)$  is the electron mean free path of photoelectrons.

The information on thermal vibrations can be extracted from fitting theoretical XAFS signals to experimental XAFS signals via several defined parameters [7]. Still, thermal disorders are sensitive to XAFS oscillations and cause anharmonic effects [5], as seen in Figure 1. It is observable that the anharmonicity of the XAFS oscillation is significant, as observed via the peak shifts and their heights [8], so thermal disorders should be considered in the XAFS signal analysis.

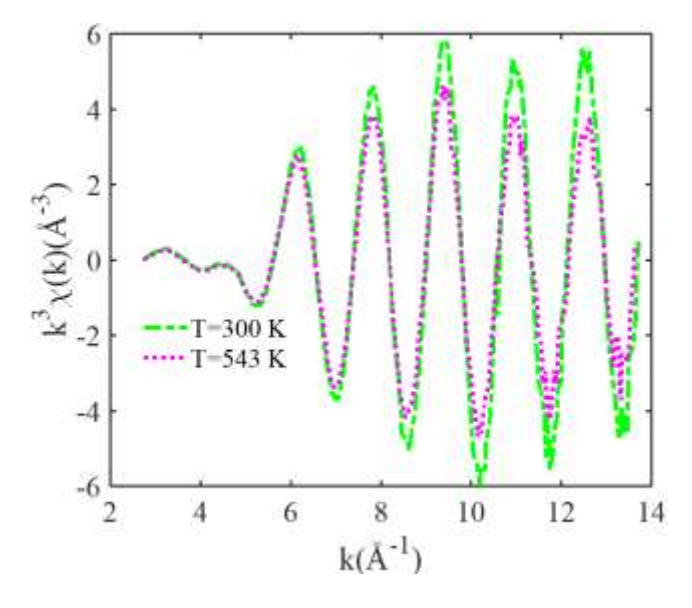


Figure 1. The K-edge XAFS signals  $k^3 \chi(k,T)$  of Br<sub>2</sub> were measured at various temperatures [6].

Nowadays, gaseous bromine (Br<sub>2</sub>) has been widely used in producing crucial materials, such as flame retardants, chemical intermediates, pharmaceuticals, insecticides, dyestuffs, and agricultural chemicals [9]. Meanwhile, the  $2^{nd}$ ,  $3^{rd}$ , and  $4^{th}$  XAFS cumulants of Br<sub>2</sub> in the temperature-dependent were obtained from the experimental data and path-integral effective-potential (PIEP) method by

Yokoyama [10]. Herein, the experimental XAFS data at 300 K, 363 K, 423 K, 483 K, and 543 K are measured at the Institute of Materials Structure Science (IMSS), Tsukuba, Japan [6, 10]. Then, the 1<sup>st</sup> XAFS cumulant of Br<sub>2</sub> was also calculated in the temperature-dependent from the PIEP method by Hai & Hieu [11]. Still, the calculated expressions cannot be obtained in explicit forms using this method.

Recently, in analyzing the anharmonic XAFS data analysis, some suitable theoretical models have been developed using suitable statistical theories based on the correlated Debye (CD) and correlated Einstein (CE) models [12-15]. An anharmonic correlated Debye (ACD) can effectively consider the phonon-dispersion effect with variable frequencies to describe the acoustic phonon branch in crystals [13, 14]. Still, its limitation is that the anharmonic EXAFS cumulants are not obtained in explicit expressions, so it takes a lot of computational effort to perform the anharmonic EXAFS data analysis. Meanwhile, a classical statistical theory within the correlated Einstein model (hereinafter referred to as the CACE model) has been employed to effectively process the XAFS cumulants of matters [8, 15]. This model uses only one effective frequency to describe thermal vibrations, but it is very convenient for analyzing anharmonic XAFS data. This is because this model allows temperature-dependent XAFS cumulants to be expressed in simple and explicit forms [16]. Still, it has not yet been applied to analyze the high-order XAFS cumulants of Br<sub>2</sub> under the influence of thermal disorder. Hence, analyzing temperature-dependent high-order XAFS cumulants of Br<sub>2</sub> using the CACE model will be essential to optimize the analytical technique of the experimental XAFS data.

#### 2. Formalism and Calculation Model

In the cumulants expansion approach, the accuracy of anharmonic XAFS data analysis can be improved by extending the anharmonic XAFS signal in approximation up to the 4<sup>th</sup> order [5]. The low-order moments of the radial pair distribution (RPD) function  $\rho(r,T)$  are directly linked to the temperature-dependent XAFS cumulants [17], so these moments can be used to express the first four XAFS cumulants in analyzing the anharmonic XAFS data as follows [6].

$$\sigma^{(1)} = \langle r \rangle - r_0 = \langle x \rangle, \tag{3}$$

$$\sigma^{(2)} \equiv \sigma^2 = \left\langle \left( r - \left\langle r \right\rangle \right)^2 \right\rangle = \left\langle x^2 \right\rangle - \left\langle x \right\rangle^2, \tag{4}$$

$$\sigma^{(3)} = \left\langle \left( x - \left\langle x \right\rangle \right)^3 \right\rangle = \left\langle x^3 \right\rangle - 3 \left\langle x^2 \right\rangle \left\langle x \right\rangle + 2 \left\langle x \right\rangle^3, \tag{5}$$

$$\sigma^{(4)} = \left\langle \left( x - \langle x \rangle \right)^4 \right\rangle - 3 \left[ \left\langle \left( x - \langle x \rangle \right)^2 \right\rangle \right]^2 = \left\langle x^4 \right\rangle + 12 \left\langle x^2 \right\rangle \left\langle x \right\rangle^2 - 3 \left\langle x^2 \right\rangle^2 - 4 \left\langle x^3 \right\rangle \left\langle x \right\rangle - 6 \left\langle x \right\rangle^4, \quad (6)$$

where  $x = r - r_0$  is the deviation interatomic distance from the equilibrium position, and cumulants  $\sigma^{(1)}$ ,  $\sigma^{(2)}$ ,  $\sigma^{(3)}$ , and  $\sigma^{(4)}$  describes the centroid, variance, asymmetry, and flatness of the RPD function, respectively.

Normally, one needs to determine an anharmonic effective (AE) potential from the atomic interaction (AI) potential of the single bond (SB) pairs in the crystal lattice, which is used to identify the thermodynamic parameters of the system [8]. After ignoring the constant contribution in the approximate expansion to the 4<sup>th</sup> order, the AE potential can be presented in the form [6]:

$$V_{eff}(x) = \frac{1}{2}k_{eff}x^2 - k_3x^3 + k_4x^4,$$
(7)

where  $k_{\rm eff}$  is an effective force constant,  $k_{\rm 3}$  and  $k_{\rm 4}$  are the anharmonic force constants.

In the correlated Einstein model theory reported by Hung et al. [18], each atomic thermal vibration can be processed as a phonon and characterized via the correlated Einstein frequency  $\omega_E$  and temperature  $\theta_E$  [19]. Utilizing the effective force constant, these parameters of Br<sub>2</sub> can be defined as follows:

$$\omega_E = \sqrt{\frac{k_{eff}}{\mu}} \,, \tag{8}$$

$$\theta_E = \frac{h\omega_E}{k_B},\tag{9}$$

where  $k_B$  is the Boltzmann constant and h is the reduced Planck constant.

In the classical statistical theory processed by Stern *et al.*, the moments  $\langle x^k \rangle$  can be identified from the 3<sup>rd</sup>-order approximation of the thermal average [16]:

$$\langle x^{k} \rangle = \frac{\int_{-\infty}^{\infty} x^{k} \exp\left[-\frac{V_{eff}(x)}{k_{B}T}\right] dx}{\int_{-\infty}^{\infty} \exp\left[-\frac{V_{eff}(x)}{k_{B}T}\right] dx} \approx \frac{\int_{-\infty}^{\infty} x^{k} \exp\left(\frac{-k_{eff}x^{2}}{2k_{B}T}\right) \left\{\sum_{n=0}^{3} \frac{1}{n!} \left(\frac{k_{3}x^{3} - k_{4}x^{4}}{k_{B}T}\right)^{k}\right\} dx}{\int_{-\infty}^{\infty} \exp\left(\frac{-k_{eff}x^{2}}{2k_{B}T}\right) \left\{\sum_{n=0}^{3} \frac{1}{n!} \left(\frac{k_{3}x^{3} - k_{4}x^{4}}{k_{B}T}\right)^{k}\right\} dx} . \quad (10)$$

Utilizing Eqs. (3)-(6) to calculate anharmonic XAFS cumulants in the temperature dependence based on Eq. (10) in the CACE model, we obtain the following result:

$$\sigma^{(1)} \approx \frac{3k_3k_BT}{k_{eff}^2} \left[ 1 - \frac{k_BT}{k_{eff}^2} \left( 32k_4 - \frac{45k_3^2}{k_{eff}} \right) \right]; \frac{3k_3k_BT}{k_{eff}^2}, \tag{11}$$

$$\sigma^{(2)} \approx \frac{k_B T}{k_{eff}} \left[ 1 - \frac{12k_B T}{k_{eff}^2} \left( k_4 - \frac{3k_3^2}{k_{eff}} \right) \right]; \frac{k_B T}{k_{eff}}, \tag{12}$$

$$\sigma^{(3)} \approx \frac{6k_3 (k_B T)^2}{k_{eff}^3} \left[ 1 - \frac{12k_B T}{k_{eff}^2} \left( 7k_4 - \frac{12k_3^2}{k_{eff}} \right) \right]; \frac{6k_3 (k_B T)^2}{k_{eff}^3}, \tag{13}$$

$$\sigma^{(4)} \approx \frac{12(k_B T)^3}{k_{eff}^4} \left( -2k_4 + \frac{9k_3^2}{k_{eff}} \right) - \frac{9(k_B T)^4}{k_{eff}^6} \left( 48k_4^2 - \frac{1288k_3^2 k_4}{k_{eff}} + \frac{2169k_3^4}{k_{eff}^2} \right); \quad \frac{12(k_B T)^3}{k_{eff}^4} \left( -2k_4 + \frac{9k_3^2}{k_{eff}} \right). \quad (14)$$

Thus, the temperature-dependent XAFS cumulants of Br<sub>2</sub> have been efficiently calculated under the influence of thermal disorder by extending the CACE model. The obtained expressions from the present model are in simple and explicit forms, and they can meet all basic properties in temperature

dependence. These expressions show the influence of anharmonic effects on the classical limit at high temperatures and indicate that the analytic expressions of high-order XAFS cumulants are very helpful for processing the anharmonic XAFS signals.

#### 3. Results and Discussions

In this section, the obtained expressions in Sec. 2 are used to calculate the numerical results of Br<sub>2</sub> based on its basic physical parameters. The calculations use local force constants  $k_{e\!f\!f}=15.349\,\mathrm{eV}\text{Å}^{-2}$ ,  $k_3=10.961\,\mathrm{eV}\text{Å}^{-3}$ , and  $k_4=6.604\,\mathrm{eV}\text{Å}^{-4}$  identified by Herzberg & Huber [20]. The obtained numerical results of the XAFS cumulants are determined at temperatures from 0 to 600 K. Our obtained results from the present CACE model are compared with those obtained from the PIEP method [10, 11] and experiment [10], in which the experimental XAFS data at 300 K, 363 K, 423 K, 483 K, and 543 K are performed by Yokoyama et al. at the Beamline 10B in the Photon Factory of the IMSS, Tsukuba, Japan [6, 10]. The numerical results are presented below.

The correlated Einstein frequency  $\omega_E$  and temperature  $\theta_E$  describe the power of atomic thermal vibrations, which are calculated by Eqs. (8)-(9) with the atomic mass  $m=79.904\,\mathrm{u}$ . Our calculated results from the present CACE model obtained are  $\theta_E$ ; 465 K and  $\omega_E$ ; 6.09.  $10^{13}\,\mathrm{Hz}$ .

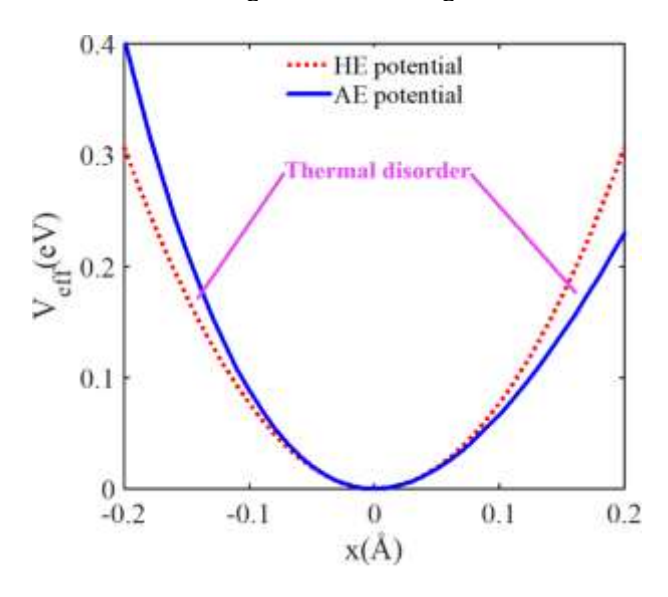


Figure 2. The position-dependent AE and harmonic effective (HE) potentials of  $Br_2$  are obtained from the present CACE model.

The AE and HE potentials of Br<sub>2</sub> at positions from - 0.2 to 0.2 Å are illustrated in Figure 2. Our obtained result from the present CACE model is calculated by Eq. (7) with the above force constants. Herein, the AE potential considers  $4^{th}$ -order terms, while the HE potential only considers  $2^{nd}$ -order terms in Eq. (7). It is observable that the obtained results indicate that the plot presenting the asymmetry of the AE potential, in which the values at the negative positions (x < 0) are is bigger than those at the positive positions (x > 0) of the same magnitude, as seen in Figure 2.

Table 1. The AE and HE potentials of Br<sub>2</sub> are obtained from the present CACE model.

Quantity	Value										
x (Å)	- 0.200	- 0.150	- 0.100	- 0.050	0	0.050	0.100	0.150	0.200		
V <sub>eff</sub> (eV) <sup>a</sup>	0.405	0.213	0.088	0.021	0	0.018	0.066	0.139	0.230		
$V_{eff}$ (eV) <sup>b</sup>	0.307	0.173	0.077	0.019	0	0.019	0.077	0.173	0.307		
<sup>a</sup> The AE potential is obtained from the present CACE model.											
<sup>b</sup> The HE potential is obtained from the present CACE model.											

The obtained values of the AE and HE potentials are given in Table 1. It is observable that the further from the equilibrium position, the AE potential is influenced more strongly by the anharmonic effect caused by terms  $(-k_3x^3)$  and  $(k_4x^4)$ , as seen in Table 1.

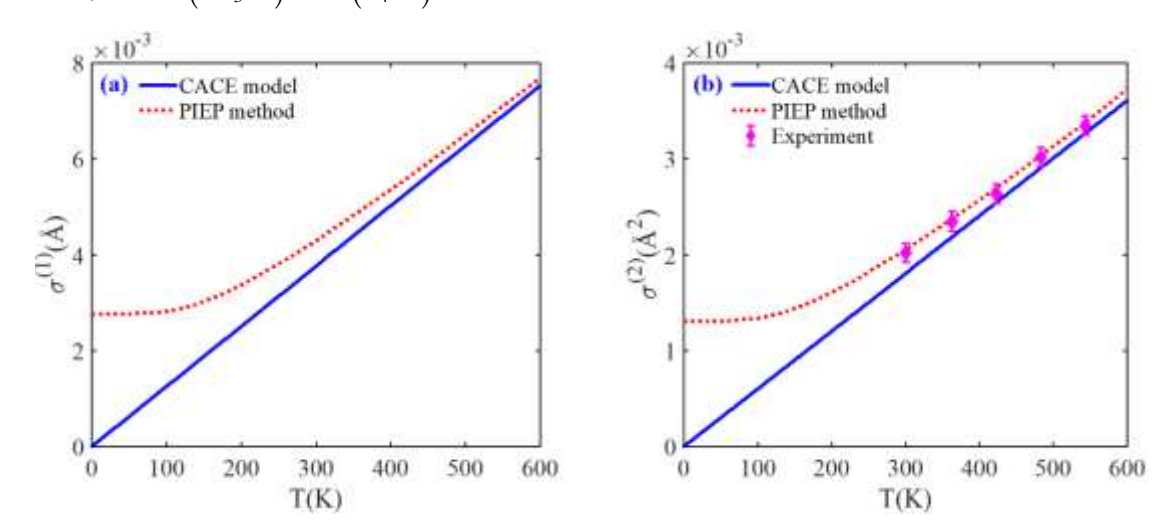


Figure 3. The temperature-dependent of the (a) 1<sup>st</sup> and (b) 2<sup>nd</sup> cumulants of Br<sub>2</sub> are obtained using the present CACE model, PIEP method [10, 11], and experiment [10].

The (a) 1<sup>st</sup> cumulant  $\sigma^{(1)}(T)$  and (b) 2<sup>nd</sup> cumulant  $\sigma^2(T)$  of Br<sub>2</sub> at temperatures from 0 to 600 K are illustrated in Figure 3. Our obtained results using the present CACE model are calculated by Eqs. (11)-(12). It is observable that our results fit with those obtained from the PIEP method [10, 11] and experiment [10] in the high-temperature (HT) range. Our results are zero as the temperature goes to the zero-point (ZP) because the present CACE model only uses a classical statistical theory and cannot calculate the quantum effects like the PIEP method [10, 11]. The present CACE model cannot work well in the low-temperature (LT) range. Still, it works correctly at room temperature, especially at temperatures higher than the correlated Einstein temperature  $\theta_E$ , as seen in Figure 3.

The (a)  $3^{rd}$  cumulant  $\sigma^{(3)}(T)$  and (b)  $4^{th}$  cumulant  $\sigma^{(4)}(T)$  of Br<sub>2</sub> at temperatures from 0 to 600 K are illustrated in Figure 4. Our obtained results from the present CACE model are calculated by Eqs. (13)-(14). It is observable that our results fit well with those obtained from the PIEP method [10] and experiment [10], especially at not-too-low temperatures. However, the present CACE model still works well for  $3^{rd}$  and  $4^{th}$  order cumulants in the LT range. This is because the contribution of quantum effects is negligible to the high-order cumulants at low temperatures, while the anharmonic effect is more evident, as seen in Figure 4.

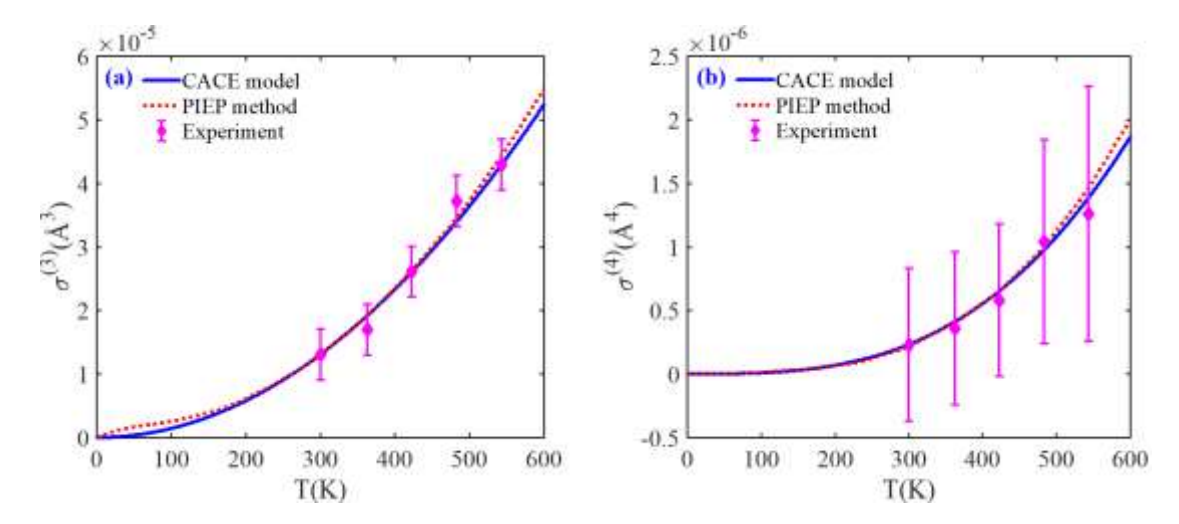


Figure 4. The temperature-dependent of the (a)  $3^{rd}$  and (b)  $4^{th}$  cumulants of  $Br_2$  are obtained from the present CACE model, PIEP method [10-11], and experiment [10].

Table 2. The XAFS cumulants of Br<sub>2</sub> are obtained from the present CACE model, PIEP method, and experiment

Method	<i>T</i> (K)	$\sigma^{(1)} (\times 10^{-2} \text{Å})$	$\sigma^{(2)} (\times 10^{-2} \text{Å}^2)$	$\sigma^{(3)}(\times 10^{-4}  \text{Å}^3)$	$\sigma^{(4)} (\times 10^{-5}  \text{Å}^4)$
CACE model <sup>a</sup>	300	0.37	0.18	0.13	0.02
	363	0.45	0.22	0.19	0.04
	423	0.53	0.25	0.26	0.07
	483	0.60	0.29	0.34	0.10
	543	0.67	0.32	0.43	0.14
PIEP method <sup>c</sup>	300	0.44	0.21	0.13	0.02
	363	0.50	0.24	0.19	0.04
	423	0.56	0.27	0.26	0.07
	483	0.63	0.30	0.35	0.10
	543	0.70	0.34	0.44	0.15
Experiment <sup>d</sup>	300		$0.20 \pm 0.01$	$0.13 \pm 0.04$	$0.02 \pm 0.06$
	363		$0.23 \pm 0.01$	$0.17 \pm 0.04$	$0.04 \pm 0.06$
	423		$0.26 \pm 0.01$	$0.26 \pm 0.04$	$0.06 \pm 0.06$
	483		$0.30 \pm 0.01$	$0.37 \pm 0.04$	$0.11 \pm 0.08$
	543		$0.34 \pm 0.01$	$0.43 \pm 0.04$	$0.13 \pm 0.10$

<sup>&</sup>lt;sup>a</sup>Our obtained values are calculated from the present CACE model.

The values of the XAFS cumulants of Br<sub>2</sub> at several temperatures are given in Table 2. It is observable that although the present CACE model gives small values and is not suitable at low temperatures in comparison with the obtained values from the PIEP method [8-9] and experiment [8], it still agrees well in the temperature range  $T \ge \theta_E$  even at room temperature, particularly for high-order XAFS cumulants, as seen in Table 2.

<sup>&</sup>lt;sup>c</sup>The obtained values are calculated from the PIEP method [10-11].

<sup>&</sup>lt;sup>d</sup>The obtained values are measured from the experiment [10].

Thus, the first four XAFS cumulants of Br<sub>2</sub> are obtained from the present CACE model, which can satisfy fundamental properties in comparison with the PIEP method and experiment at not-too-low temperatures, particularly above the correlated Einstein temperature. These results describe thermal vibration contributions influencing the classical limit via anharmonic effects at high temperatures, in which the anharmonicity of the XAFS signal arises from about room temperature.

#### 4. Conclusions

In this work, we have effectively applied the present CACE model to calculate the temperature-dependent high-odder XAFS cumulants of  $Br_2$  under the influence of thermal disorder. The obtained expressions of the first four XAFS cumulants are in simple and explicit forms of the temperature T. These results can meet all basic properties in the temperature dependence and can also show the anharmonicity of the XAFS signal at high temperatures. Our numerical results of  $Br_2$  fit with those obtained from the PIEP method and experiment at high temperatures, even at room temperature, particularly for high-order cumulants. The agreement between our results and the results of other works in the comparisons indicates the usefulness of this calculation model. This model can be applied to analyze experimental XAFS cumulants of other gases from above the temperature  $\theta_E$  to just before the melting temperature  $\theta_m$ .

## Acknowledgments

This research is funded by the Vietnam National Foundation for Science and Technology Development (NAFOSTED) under grant number 103.01-2023.32.

### References

- [1] C. W. Pao et al., The New X-ray Absorption Fine-Structure Beamline with Sub-second Time Resolution at the Taiwan Photon Source, Journal of Synchrotron Radiation, Vol. 28, No. 3, 2021, pp. 930-938, https://doi.org/10.1107/S1600577521001740.
- [2] T. Yokoyama, S. Chaveanghong, Anharmonicity in Elastic Constants and Extended X-ray-absorption Fine Structure Cumulants, Physical Review Materials, Vol. 3, 2019, pp. 033607, https://doi.org/10.1103/PhysRevMaterials.3.033607.
- [3] P. Fornasini, R. Grisenti, M. Dapiaggi, G. Postini, Local Structural Distortions in SnTe Investigated by EXAFS, Journal of Physics: Condensed Matter, Vol. 33, 2021, pp. 295404, https://doi.org/10.1088/1361-648X/ac0082.
- [4] P. A. Lee, P. H. Citrin, P. Eisenberger, B. M. Kincaid, Extended X-ray Absorption Fine Structure-its Strengths and Limitations as A Structural Tool, Reviews of Modern Physics, Vol. 53, No. 4, 1981, pp. 769-806, https://doi.org/10.1103/RevModPhys.53.769.
- [5] G. Bunker, Application of the Ratio Method of EXAFS Analysis to Disordered Systems, Instruments and Methods in Physics Research, Vol. 207, No. 3. 1983, pp. 437-444, https://doi.org/10.1016/0167-5087(83)90655-5.
- [6] T. Yokoyama, K. Kobayashi, T. Ohta, A. Ugawa, Anharmonic Interatomic Potentials of Diatomic and Linear Triatomic Molecules Studied by Extended X-ray Absorption Fine Structure, Physical Review B, Vol. 53, No. 10, 1996, pp. 6111-6122, https://doi.org/10.1103/PhysRevB.53.6111.
- [7] G. Dalba, P. Fornasini, M. Grazioli, Local Disorder in Crystalline and Amorphous Germanium, Physical Review B, Vol. 52, No. 15, 1995, pp. 11034-11043, https://doi.org/10.1103/PhysRevB.52.11034.
- [8] T. S. Tien, Temperature-Dependent EXAFS Debye-Waller Factor of Distorted HCP Crystals, Journal of the Physical Society of Japan, Vol. 91, No. 5, 2022, pp. 054703, https://doi.org/10.7566/JPSJ.91.054703.

- [9] K. J. Szabo, N. Selander, Organofluorine Chemistry: Synthesis, Modeling, and Applications, Wiley-VCH, Weinheim, 2021, https://doi.org/10.1002/9783527825158.
- [10] T. Yokoyama, Path-integral Effective-potential Method Applied to Extended X-ray-absorption Fine-structure Cumulants, Physical Review B, Vol. 57, No. 6, 1998, pp. 3423-3432, https://doi.org/10.1103/PhysRevB.57.3423.
- [11] H. K. Hieu, N. M. Hai, Application of Path-integral for Studying EXAFS Cumulants, Communications in Physics, Vol. 14, No. 3S1, 2014, pp. 40-44, https://doi.org/10.15625/0868-3166/24/3S1/5075.
- [12] T. S. Tien, Advances in Studies of the Temperature Dependence of the EXAFS Amplitude and Phase of FCC Crystals, Journal of Physics D: Applied Physics, Vol. 53, No. 11, 2020, pp. 315303, https://doi.org/10.1088/1361-6463/ab8249.
- [13] N. B. Duc, V. Q. Tho, T. S. Tien, D. Q. Khoa, H. K. Hieu, Pressure and Temperature Dependence of EXAFS Debye-Waller Factor Of Platinum, Radiation Physics and Chemistry, Vol. 149, 2018, pp. 61-64, https://doi.org/10.1016/j.radphyschem.2018.03.017.
- [14] T. S. Tien, L. D. Manh, N. T. M. Thuy, N. C. Toan, N. B. Trung, L.V. Hoang, Investigation of Anharmonic EXAFS Parameters of Ag Using Anharmonic Correlated Debye Model Under the Effect of Thermal Disorders, Solid State Communications, Vol. 388, 2024, pp. 115545, https://doi.org/10.1016/j.ssc.2024.115545.
- [15] T. S. Tien et al., High-order EXAFS Cumulants of Diamond Crystals Based on A Classical Anharmonic Correlated Einstein Model, Journal of Physics and Chemistry of Solids, Vol. 134, 2019, pp. 307-312, https://doi.org/10.1016/j.jpcs.2019.06.020.
- [16] E. A. Stern, P. Livins, Z. Zhang, Thermal Vibration and Melting from A Local Perspective, Physical Review B, Vol. 43, No. 11, 1991, pp. 8850-8860, https://doi.org/10.1103/PhysRevB.43.8850.
- [17] J. Freund, R. Ingalls, E. D. Crozier, Extended X-ray-absorption Fine-structure Study of Copper Under High Pressure, Physical Review B, Vol. 39, No. 17, 1989, pp. 12537-12547, https://doi.org/10.1103/PhysRevB.39.12537.
- [18] N.V. Hung, J.J. Rehr, Anharmonic correlated Einstein-model Debye-Waller factors, Physical Review B, Vol. 56, No. 1, 1997, pp. 43–46, https://doi.org/10.1103/PhysRevB.56.43.
- [19] N. V. Hung, T. S. Tien, N. B. Duc, D. Q. Vuong, High-order Expanded XAFS Debye-Waller Factors of HCP Crystals Based on Classical Anharmonic Correlated Einstein Model, Modern Physics Letters B, Vol. 28, No. 21, 2014, pp. 1450174, https://doi.org/10.1142/S0217984914501747.
- [20] K. P. Huber, G. Herzberg, Molecular Spectra and Molecular Structure, IV: Constants of Diatomic Molecules, Springer New York, New York, 1979, https://doi.org/10.1007/978-1-4757-0961-2.